Dalton Transactions

RSC Publishing

PAPER

Oxidation of copper nanoparticles in water: mechanistic insights revealed by oxygen uptake and spectroscopic methods†

Cite this: *Dalton Trans.*, 2013, **42**, 5832

Natalia L. Pacioni, Vasilisa Filippenko, Nathalie Presseau and J. C. Scaiano*

Received 27th November 2012,
Accepted 4th February 2013

DOI: 10.1039/c3dt32836h

www.rsc.org/dalton

Oxidation of aqueous ~8 nm unprotected copper nanoparticles takes place under air in approximately 2 hours at 30 °C to give Cu^{2+} as a final product through an intermediate Cu^{+} species. At 5 °C the process is about 5 times slower; similarly, vitamin C, which plays a sacrificial role, also slows down the oxidation, while CuNP catalyses the oxidation. In this work, we present a detailed analysis of the oxidation mechanism of colloidal CuNP inferred through spectroscopic methods (UV-visible and EPR) combined with oxygen uptake measurements, with emphasis on factors affecting the oxidative process.

Introduction

Great interest in copper nanoparticles (CuNP) has arisen during the last few decades due to their potential applications in electronic and optical devices,[1] as well as in the area of catalysis.[2] One of the main advantages of CuNP with respect to their gold and silver analogues is their low cost, but the main limitation is their instability under air due to oxidation. In order to prevent this process, different alternatives have been proposed including the 'capping' of nanoparticles with different stabilizers such as polyvinylpyrrolidone (PVP)[3] or different surfactants.[4,5] Nevertheless, since relatively high stabilizer concentrations are required, the stabilizer most likely modifies the chemistry of CuNP.

A rational understanding of the oxidative process becomes a priority in developing strategies for CuNP stabilization, however there are only a few literature reports devoted to the oxidation of CuNP.[5–10] For example, Yanase and Komiyama[6] followed the oxidation and reduction of CuNP on supports at temperatures in the 25–400 °C range by optical absorption and X-ray diffraction, finding that the reaction involves a fast oxidation of Cu^{0} to Cu(I) oxide followed by a slow reaction to finally render Cu(II) oxide. They also determined the value of activation energy for the last step to be 69 kJ mol^{-1}. Later, van Wijk *et al.*[7] studied the effects of particle size on the oxidation of supported CuNP with respect to temperature and pressure by X-ray photoelectron spectroscopy (XPS). They determined that at room temperature and 10 Pa, the smaller particles (4 nm) showed slower oxidation at the surface than 15 nm particles, while at 300 °C a reverse trend was observed. In both cases, also Cu^{0} was oxidized to Cu(II) oxide through an intermediate Cu(I) oxide.

Recently, Chen *et al.* investigated the self-limiting nature of the CuNP oxidation. They determined that at room temperature this phenomenon is due to internal stress caused by an oxide layer on the surface that is overcome at higher temperatures (50 °C), whereas Kanninen *et al.*[5] reported a qualitative analysis of the oxidation of ligand-stabilized CuNP in toluene at room temperature. Yabuki *et al.*[10] reported the oxidation behavior of CuNP prepared by the RF thermal plasma method by thermal gravimetry analysis (TG-DTA) between 150 and 300 °C and following the products by XRD; and observed differences in the process below and above a threshold temperature. Haddou *et al.*[9] investigated the electrochemical oxidation of copper nanoparticles in aqueous solutions in 1.0 M HNO_3 and in 1.0 M HNO_3–0.1 M KCl, and found the reaction to be quantitative and involving a two electron oxidation to Cu^{2+} in the first case and two separate one-electron steps in the second case.

In this work, we propose a mechanism for the oxidation of unprotected CuNP in water examined through a combination of experimental approaches: first by observing either the CuNP themselves or their intermediate and final product using UV-visible and electron paramagnetic resonance (EPR) spectroscopies, and second by observing the consumption of molecular oxygen as it reacts with the CuNP.

Interestingly, the second approach explores a novel application of the inhibited oxygen uptake apparatus, commonly used for the study of carbon-centered radicals and

Centre for Catalysis Research and Innovation, Department of Chemistry, University of Ottawa, 10 Marie Curie, Ottawa, K1N 6N5, Canada.
E-mail: tito@photo.chem.uottawa.ca

†Electronic supplementary information (ESI) available: Kinetics profile at different temperatures, EPR showing Cu^{2+} reduction by ascorbic acid. See DOI: 10.1039/c3dt32836h

This journal is © The Royal Society of Chemistry 2013

antioxidants.[11] Briefly, this apparatus uses a pressure transducer to detect pressure differences between the closed environments of a sample cell, where a reaction that consumes oxygen is occurring, and a reference cell, where no reaction is taking place. This instrument now shows promise for studying the reactions of nanoparticles with oxygen.

Finally, the effect of L-ascorbic acid on the CuNP oxidation will be discussed. L-Ascorbic acid is an important water soluble antioxidant *in vivo*, where it plays a role in various biological processes, such as vitamin E recycling.[12] In addition, it is well known to reduce transition metal complexes,[13] and to oxidize faster in the presence of Fe(III) and Cu(II).[14] We investigated its potential use in retarding the oxidative degradation of CuNP under air, where we observed that L-ascorbic acid protects the particles by playing a sacrificial role.

Experimental section

General details

Anhydrous $CuSO_4$, L-ascorbic acid and neocuproine hydrate were from Sigma-Aldrich and were used as received. 2-Hydroxy-1-[4-(2-hydroxyethoxy)phenyl]-2-methyl-1-propanone (I-2959) was a generous gift from Ciba Speciality Chemicals and was recrystallized from ethyl acetate prior to use. Doubly distilled deionized water was obtained from a Milli-Q system (18.2 MΩ resistance).

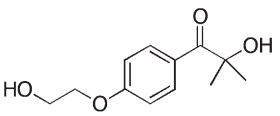

Irgacure 2959
I-2959

Copper nanoparticles were synthesized as previously reported.[15] Briefly, 3 mL of aqueous solutions containing 0.66 mM $CuSO_4$ and 1.3 mM I-2959 were deaerated by bubbling argon for 30 min through PTFE tubing attached to a needle. Samples were irradiated for 30 min using a 10 × 10 mm fused silica cuvette placed in a Luzchem LZC-4V photoreactor equipped with 14 UVA lamps and a carousel to rotate the samples during photolysis.

As synthesized CuNP were characterized by UV-visible spectroscopy in the 300–900 nm wavelength range, showing the characteristic surface plasmon resonance band (SPB) at 575 nm,[15,16] and by SEM (field emission scanning electron microscope: Jeol, JSM-7500F). The average size is 8.2 nm (s.d.: 3.1 nm). The concentration of CuNP can be estimated from these data as ~20 nM in a similar way as reported for gold nanoparticles.[17]

UV-visible measurements

Oxidation of CuNP. Generally, the samples were exposed to air upon removal of the septum from the cuvette, and a magnetic stirring bar was added to help oxygen diffusion into the solution. The UV-visible absorbance spectra were obtained in the 400–900 nm wavelength range in a Cary-50 (Varian) with a single cell Peltier temperature control accessory. CuNP oxidation was followed by monitoring the decrease in absorbance of the SPB band at 575 nm. The experiments were performed at 5 °C, 30 °C and 45 °C in the absence, as well as in the presence, of 1 mM L-ascorbic acid (**VC**).

Copper(I) detection with neocuproine. A 1.62 mg mL^{-1} 2,9-dimethyl-1,10-phenanthroline stock solution was prepared in ethanol. 100 μL of the neocuproine stock solution were added to a 1 × 1 cm quartz cuvette containing Milli-Q water (1.4 mL). Then 1.5 mL CuNP solution were added and the absorbance spectra were recorded at 30 s intervals for 30 min in the 300–900 nm range under air or under N_2 at room temperature. Measurements under an inert atmosphere were done in a glovebox (LC Technology Solutions Inc.).

Oxygen uptake determinations

An oxygen uptake apparatus was used to perform these experiments. A typical measurement was done as described below.

Cells containing 2 mL water were loaded onto the apparatus and equilibrated overnight at 30 °C. A control experiment was done with argon-purged water, to account for the pressure change sensed by the apparatus due to argon gas. Water was purged in a cuvette in the same way as the sample during CuNP synthesis, and equilibrated to 30 °C in a water bath for 5 minutes prior to injection. The sample cell was emptied, dried, and 2 mL of the argon-purged water injected into the sample cell using a syringe and PTFE needle. The slope of this control curve was subtracted from the subsequent sample runs, done on the same day.

For the CuNP measurements, the cuvette with the nanoparticles was equilibrated to 30 °C in a water bath for 5 minutes prior to injection. The sample cell was again removed, emptied, dried, and 2 mL of CuNP were injected into the sample cell.

For CuNP experiments with ascorbic acid, a stock solution of ascorbic acid was purged with argon for 30 minutes, and equilibrated to 30 °C as described above. Ascorbic acid was injected into the CuNP (usually to a final ascorbic acid concentration of 1 mM) right before starting the oxygen uptake experiment.

EPR spectroscopy of copper(II)

The EPR measurements were performed with a JEOL FA-100 X-Band EPR spectrometer (Jeol USA, Peabody, MA). The samples were run in a 0.3 mm fused quartz flat cell (Jeol Co.), at room temperature, and in the absence of oxygen.

Typical experiments were done as follows. A CuNP precursor solution (0.66 mM $CuSO_4$, 1.3 mM I-2959 in water) was prepared, then divided into two quartz cuvettes and purged with argon for 30 minutes as previously described. One cuvette was irradiated to prepare CuNP, while the other was used to run the EPR spectrum of the precursor solution. EPR spectra were also obtained for the CuNP sample and for the same CuNP sample after it was purged with O_2 for 30 minutes followed by re-purging with argon for 30 minutes.

The EPR spectra were obtained at a frequency of ~9413 MHz. The acquisition parameters were power = 5 mW,

mod. frequency = 100 kHz, mod. width = 1.0 mT, time constant = 0.03 s, and sweep time = 4 min. Usually, 3 accumulations were obtained. When using the Mn standard, the Mn peak intensity was chosen to be 500 units.

For the experiment with CuNP and **VC**, non-irradiated and CuNP runs were obtained as described above. Runs were acquired at 6, 36, 51, 66 and 96 minutes after ascorbic acid addition. EPR acquisition conditions were the same as above, except single accumulations were obtained at each time.

Results

Oxidation of copper nanoparticles

We chose to work with aqueous 8 nm CuNP, synthesized photochemically using copper sulfate as previously reported,[15] due to the desirable characteristics of these particles, such as a relatively unprotected surface, high monodispersity and shape uniformity, which are desired factors for mechanistic studies.

As synthesized, these CuNP are stable in the absence of oxygen and show the characteristic surface plasmon band (SPB) absorption at 575 nm. Once exposed to ambient conditions the colloidal solution changes colour from reddish-brown to colorless (without any precipitate) as a result of their oxidation.[15]

For a better understanding of the fate of these CuNP, different experiments were carried out. First, we followed the disappearance of the band at 575 nm upon air exposure at 30 °C with magnetic stirring. An independent experiment was done with mechanical agitation every 2 minutes. Fig. 1 (top) shows how the SPB decreases over time as an indication of CuNP consumption. The absence of any red shift in the SPB or broadening of the band indicates that neither aggregation[18] nor oxide formation are significant, since it is known that if the CuNP were surrounded by a copper oxide monolayer, they would display an additional absorption around 800 nm, something that was not observed with our samples.[6,16] Moreover, formation of oxides is not expected at the low pH that results from the synthesis of these CuNP.[15,19] Even under oxidative conditions Cu(0) reverts to Cu^{2+} in solution, rather than its oxide (*vide infra*).

Further, large variations in particle size distribution seem unlikely as the peak position remains unchanged.[20,21] On the other hand, changes in the absorbance reflect a variation in the number of particles.[21] Therefore, the extent of oxidation can be estimated in a good approximation from a plot of the absorbance at any time with respect to the initial absorbance at 575 nm.

The kinetics profile shown in Fig. 1 (bottom) at 30 °C and atmospheric pressure shows a delay time ($\Delta Abs \leq 5\%$) of ~5 min, which is independent of the stirring method (see inset), followed by the consumption of CuNP. The overall process is complete in about two and a half hours when magnetic stirring was used, and approximately in an hour and a half with mechanical stirring. Decreasing the temperature to 5 °C slowed down the process, and increasing it to 45 °C showed the steepest slope (ESI†). Table 1 shows the estimated half-lives at different temperatures.

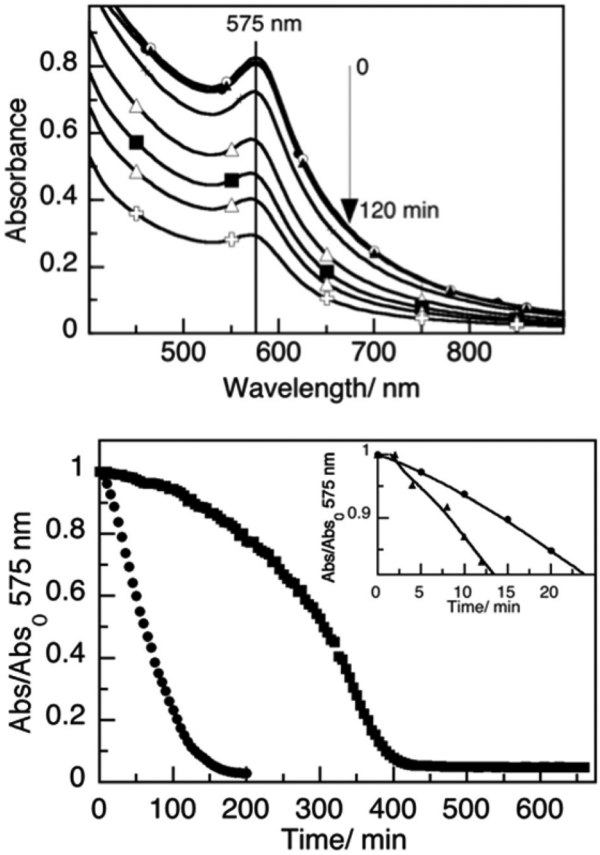

Fig. 1 (Top) UV-visible absorbance spectra of CuNP synthesized from 0.66 mM $CuSO_4$ upon exposure to air at 30 °C at selected times. (Bottom) Relative absorbance at 575 nm in the absence (●) or presence (■) of 1 mM ascorbic acid at 30 °C. Inset shows the differences found in the oxidation process depending on the type of stirring; (●) magnetic stirring or (▲) vigorous shaking every 2 min.

Table 1 Half-life for the oxidation of CuNP at different temperatures in the absence or presence of 1 mM ascorbic acid (**VC**)

Temperature/°C	$t_{1/2}$ [a]/min	
	No **VC**	**VC** 1 mM
5	481	1144
30	60 (34)[b]	308
45	30	122

[a] Half-life estimated from kinetics profiles as the time where the SPB absorption at 575 nm decreased by 50%. [b] Corresponds to mechanical stirring.

In order to determine if the kinetic differences in Fig. 1 (bottom) and in Table 1 were due to the consumption of oxygen, we performed oxygen uptake measurements using a method that is widely employed in antioxidant activity studies.[11] We successfully detected that throughout CuNP oxidation, oxygen is consumed at a 0.15 μM s^{-1} rate, with a total O_2 consumption of *ca.* 0.20 mM when using CuNP prepared from 0.66 mM copper sulfate.

 This journal is © The Royal Society of Chemistry 2013

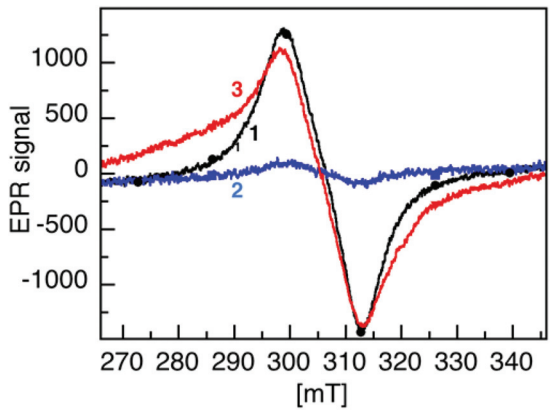

Fig. 2 EPR spectra of 0.66 mM $CuSO_4$ containing 1.3 mM I-2959 reaction mixture; non-irradiated (1, black); after 30 min UVA irradiation (2, blue) followed by 30 min O_2 purging (3, red). All spectra were recorded at room temperature under argon.

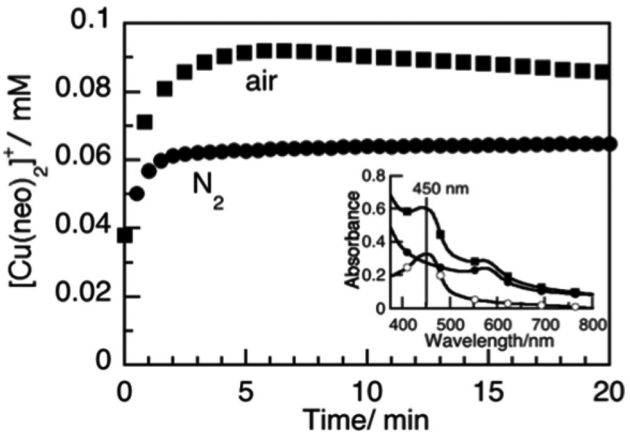

Fig. 3 Formation of $[Cu(neo)_2]^+$ over time calculated from ΔAbs values at 450 nm (ε: 7.4 mM^{-1} cm^{-1}) under air or N_2 at room temperature. Reaction conditions were ~10 nM CuNP and 54 μg mL^{-1} *neo*. (*Inset*) Absorbance spectra of 10 nM CuNP in the presence (■), absence (●) of *neo*, and the corresponding difference spectrum (○).

As mentioned above, since metal oxide formation is likely not to occur under our experimental conditions, the oxidation product is probably the reversion to Cu^{2+}. To confirm this hypothesis, we performed electron paramagnetic resonance (EPR) experiments in order to monitor the Cu^{2+} throughout the CuNP formation and oxidation process. For example, in Fig. 2 we can see the EPR spectra showing the Cu^{2+} signal before and after the CuNP synthesis, showing a signal for residual Cu^{2+} and the total regeneration of the Cu^{2+} signal after CuNP oxidation. We also attempted to quantify the amount of residual Cu^{2+} after the synthesis (blue trace in Fig. 2), by using the integrated signal, getting a value of 5 μM. We note that the residual Cu^{2+} usually varies from batch to batch.

Under the conditions mentioned above, a *g*-value of 2.212 was found for Cu^{2+} which is comparable to those reported for other copper(II) compounds in solution at room temperature.[22] Thus, we confirmed that the final product is Cu^{2+} in solution.

We also wondered if as happens in the synthesis,[15] the oxidation of CuNP could involve Cu^+ as an intermediate. For this purpose, we used neocuproine (*neo*) as a specific Cu^+ sensor (Chart 1). It is well known that *neo* forms a very stable complex with Cu^+ ($[Cu(neo)_2]^+$), which strongly absorbs at 450 nm (ε_{H_2O}: 7400 M^{-1} cm^{-1}), making it readily detectable at levels as low as 0.03 μg of copper.[23] Thus, we recorded the absorption spectrum upon time for the oxidation of ~10 nM CuNP under air in the presence and absence of neocuproine (54 μg mL^{-1}). We also performed the experiment under anaerobic conditions as a control. From the difference between the spectra at time zero (Fig. 3 inset) we calculated a residual $[Cu^+]$ of ~0.038 mM in both cases (aerobic and anaerobic conditions). Under anaerobic conditions, we observed reduced formation of the complex; this may be due to limited oxidation of CuNP promoted by the complex formation. However, the amount of complex formed is 1.5 times larger under aerobic conditions, indicating that during the oxidation of CuNP the intermediate Cu^+ is also obtained.

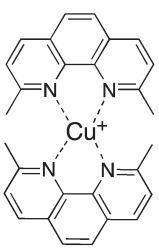

Chart 1 Structure of the complex formed between Cu^+ and neocuproine.

Effect of L-ascorbic acid in the CuNP oxidation

Addition of L-ascorbic acid (vitamin C, **VC**), a well-known water soluble radical scavenger, led to a delay in the oxidation process as seen in Fig. 1 (bottom), increasing the half-life by at least five times (Table 1). In order to infer more about the reaction mechanism when **VC** is present, EPR and oxygen uptake measurements were also performed. Note in Fig. 1 that the rate of consumption once **VC** has been depleted (*e.g.* at absorbances < 0.2) is essentially the same for both curves.

First, the residual Cu^{2+} signal was followed by EPR up to 96 min after the addition of **VC** under N_2. We observed a decrease in the Cu^{2+} signal, and therefore in Cu^{2+} concentration (see ESI†). Moreover, we also found that **VC** is able to reduce Cu^{2+} to Cu^+ in the absence of oxygen by detecting the $[Cu(neo)_2]^+$ complex, which is not detected in the absence of **VC**. This indicates that under anaerobic conditions, **VC** is able to react with Cu^{2+}, and most likely reduces it to Cu^+, increasing its concentration and thus promoting the disproportionation reaction. This means that under aerobic conditions, **VC** could also be stabilizing the CuNP by favouring recovery of Cu^0 that could attach to existing CuNP, thus effectively delaying CuNP oxidation.

To our surprise, when we did the oxygen uptake determination (Fig. 4A), the oxygen consumption rate during the CuNP oxidation in the presence of 1 mM **VC** was 2.03 μM s^{-1}, ~15 times larger than in the absence of **VC**, and the total

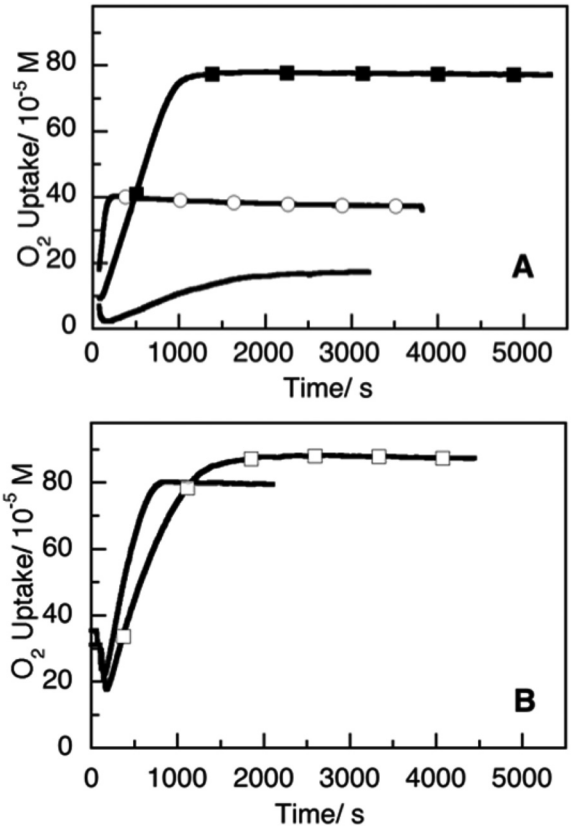

Fig. 4 Oxygen uptake of (A) CuNP in the absence (—) and presence of 1 mM **VC** (■), and non-irradiated precursor reaction mixture ([Cu^{2+}] = 0.66 mM) in the presence of 1 mM **VC** (○); (B) samples containing 1 mM VC and either CuNP (□) or 0.076 mM Cu^{2+} (—). All reactions were performed at 30 °C.

amount of O_2 consumed was almost 5 times more than for CuNP alone, indicating the possibility of a sacrificial role of **VC** in the observed CuNP 'stabilization'. Further, the O_2 consumption rate by 1 mM **VC** in the absence of CuNP was determined as approximately 0.1 μM s^{-1}, which would indicate a 'catalytic' effect by CuNP on the auto-oxidation of **VC**. It is well known that Cu(II) and Fe(III) are efficient catalysts of **VC** auto-oxidation.[14] Our results indicate that CuNP may also have the capability to catalyze this reaction.

Several oxygen uptake experiments were carried out to explore the **VC** oxidation with CuNP and Cu^{2+} (Fig. 4). As seen in Fig. 4A, Cu^{2+} is faster than CuNP in catalyzing **VC** oxidation. Nevertheless, it is important to note that the CuNP concentration as synthesized is approximately 20 nM: 30 000 times smaller than the Cu^{2+} concentration. Thus, in order to verify which species plays the key role in **VC** oxidation, we carried out several oxygen uptake experiments varying the Cu^{2+} concentration (Table 2). These experiments show two facts:

(i) the O_2 consumption is relatively constant, and

(ii) the O_2 uptake rate depends on the [Cu^{2+}] in the concentration range studied.

We have already mentioned that the residual Cu^{2+} found varied from batch to batch, so we ran an oxygen uptake experiment of a CuNP solution whose residual Cu^{2+} concentration was previously determined by EPR as 0.076 mM and compared to the one performed in the presence of 0.076 mM Cu^{2+} (Fig. 4B). Under these conditions the oxygen consumption was faster when Cu^{2+} was used.

Table 2 Effect of [Cu^{2+}] in the oxygen uptake rate by aqueous 1 mM **VC**

[$CuSO_4$]/mM	O_2 uptake rate/μM s^{-1}	O_2 consumed/mM
0	0.04	N/A
0.10	1.55	0.64
0.20	3.33	0.63
0.33	4.14	0.60
0.66	6.03	0.61
1.32	7.81	0.55

Discussion

Our results provide evidence of key indicators to understand the mechanism of the oxidation of unprotected aqueous CuNP:

(a) there is an initial short period that is independent of the stirring method, followed by the observation that the number of particles decreases under air without any precipitation;

(b) the final product is Cu^{2+};

(c) O_2 is being consumed during the reaction;

(d) the process involves initial oxidation to Cu^{+};

(e) there is some residual Cu^{+} and Cu^{2+} after the synthesis of CuNP;

(f) addition of L-ascorbic acid to the system slows down the consumption of CuNP;

(g) the oxidation of **VC** is catalysed by addition of CuNP (although likely due to copper ions in solution); and

(h) **VC** readily reduces Cu^{2+} to Cu^{+}.

The absence of any precipitate and the complete recovery of the Cu^{2+} signal in EPR rule out the formation of cuprous or cupric oxides, in contrast with the fate of supported CuNP under air.[6–8] Thus, under our experimental conditions after initial oxidation to get an intermediate Cu^{+}, the reaction follows the complex chemistry of Cu^{+} with oxygen.[24] Our interpretation of the reaction is presented in the mechanism shown in Scheme 1. We note that this mechanism is a simplified view of the overall oxidative process, with only the main steps highlighted here.

(i) First, it is probable that residual Cu^{+} reacts with O_2 to give the unstable adduct CuO_2^{+} that decomposes rapidly to give Cu^{2+} and $O_2^{-\cdot}$ (or $HO_2^{\cdot}$). This would explain the short delay observed before starting the actual consumption of CuNP.

(ii) Once the reactive surface of CuNP interacts with O_2, Cu^{+} is formed and it will follow point (i) as described to give Cu^{2+} as the final product (red arrows in Scheme 1).

When ascorbic acid is added, the overall reaction is retarded (black arrows in Scheme 1). This is attributed to additional paths involving (i) reduction of residual Cu^{2+} back to Cu^{+}, facilitating the disproportionation reaction (blue arrows in Scheme 1) to regenerate Cu(0). Therefore, the CuNP oxidation is delayed by additional formation of Cu^{0}, which

 This journal is © The Royal Society of Chemistry 2013

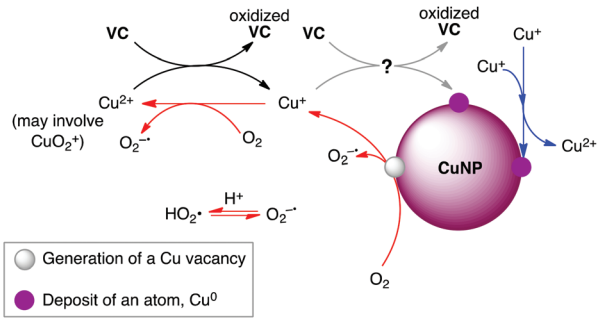

Scheme 1 Proposed pathways involved in the oxidation mechanism of aqueous CuNP under aerobic conditions. **VC** means ascorbic acid. In the absence of **VC** the red arrows show the oxidation mechanism, while blue arrows show Cu(I) disproportionation, that can occur in all cases. The top region with black arrows shows the proposed mechanism for **VC** action, involving recovery of Cu(0); this last section is shown in grey (with a question mark) as our study cannot rule out that disproportionation is the only mechanism for Cu(0) recovery.

may be able to bind to existing CuNP (that effectively behaves as a seed), and (ii) a catalytic cycle for the ascorbic oxidation is established as shown in Scheme 1. In this way, the CuNP lifetime is extended, while ascorbic acid plays a sacrificial role. Finally, the Cu^{2+} in this scenario catalyzes the oxidation of **VC**, which is consistent with our results. Thus, a controlled release of Cu^{+} or Cu^{2+} from CuNP might be promising in catalysis of reactions such as in those involved in click chemistry.[25] The fate of $HO_2^{\cdot}$ (or $O_2^{-\cdot}$) is likely trapping by **VC**, when present, or otherwise disproportionation to give H_2O_2.

Conclusions

Spherical CuNP, synthesized photochemically from aqueous copper sulphate and I-2959, are easily oxidized under air at atmospheric pressure to give aqueous Cu^{2+} as the product, rather than copper oxides. The oxidation presents a complex mechanism with Cu^{+} as the intermediate. The overall process could be retarded either by keeping the CuNP at low temperature or by adding L-ascorbic acid as a sacrificial stabilizer. Both residual and released Cu^{2+} are able to catalyse the oxidation of L-ascorbic acid, that plays a key role in extending the lifetime of CuNP by reducing Cu^{2+} back to Cu^{+}, thus permitting the CuNP to rebuild *via* Cu(0) regeneration.

Acknowledgements

We thank the Natural Sciences and Engineering Research Council of Canada for generous support.

Notes and references

1 F. E. Kruis, H. Fissan and A. Peled, *J. Aerosol Sci.*, 1998, **29**, 511–535; X. Liu, W. Cai and H. Bi, *J. Mater. Res.*, 2002, **17**, 1125–1128.
2 P. Singh, A. Katyal, R. Kalra and R. Chandra, *Catal. Commun.*, 2008, **9**, 1618–1623; S. Bhadra, A. Saha and B. Ranu, *Green Chem.*, 2008, **10**, 1224.
3 C. Wu, B. Mosher and T. Zeng, *J. Nanopart. Res.*, 2006, **8**, 965–969.
4 S. Wu, *J. Colloid Interface Sci.*, 2004, **273**, 165–169.
5 P. Kanninen, C. Johans, J. Merta and K. Kontturi, *J. Colloid Interface Sci.*, 2008, **318**, 88–95.
6 A. Yanase and H. Komiyama, *Surf. Sci.*, 1991, **248**, 11–19.
7 R. van Wijk, P. C. Gorts, A. J. M. Mens, O. L. J. Gijzeman, F. H. P. M. Habraken and J. W. Geus, *Appl. Surf. Sci.*, 1995, **90**, 261–169.
8 C.-H. Chen, T. Yamaguchi, K.-I. Sugawara and K. Koga, *J. Phys. Chem. B*, 2005, **109**, 20669–20672.
9 B. Haddou, N. Rees and R. Compton, *Phys. Chem. Chem. Phys.*, 2012, **14**, 13612.
10 A. Yabuki and S. Tanaka, *Mater. Res. Bull.*, 2011, **46**, 2323–2327.
11 M. Frenette, P. D. MacLean, L. R. C. Barclay and J. C. Scaiano, *J. Am. Chem. Soc.*, 2006, **128**, 16432; V. Filippenko, M. Frenette and J. C. Scaiano, *Org. Lett.*, 2009, **11**, 3634–3637; L. R. C. Barclay, *Can. J. Chem.*, 1993, **71**, 1–16.
12 E. Cadenas and L. Packer, *Handbook of Antioxidants*, Marcel Dekker Inc., Handbook of Antioxidants, 1996.
13 I. Fabian and V. Csordas, in *Advances in Inorganic Chemistry*, ed. R. van Eldik and C. D. Hurbard, Elsevier Science, USA, 2003, pp. 395–459.
14 D. Miller, G. Buettner and S. Aust, *Free Radicals Biol. Med.*, 1990, **8**, 95–108; E. V. Shtamm, A. P. Purmal and Y. I. Skurlatov, *Int. J. Chem. Kinet.*, 1979, **XI**, 461–494; M. Hynes and D. Kelly, *J. Chem. Soc., Chem. Commun.*, 1988, 849–850.
15 N. L. Pacioni, A. Pardoe, K. L. McGilvray, M. N. Chretien and J. C. Scaiano, *Photochem. Photobiol. Sci.*, 2010, **9**, 766–774.
16 M. P. Pileni, *New J. Chem.*, 1998, 693–702.
17 D. J. Lewis, T. M. Day, J. V. MacPherson and Z. Pikramenou, *Chem. Commun.*, 2006, 1433–1435; N. L. Pacioni, M. Gonzalez-Bejar, E. Alarcon, K. L. McGilvray and J. C. Scaiano, *J. Am. Chem. Soc.*, 2010, **132**, 6298–6299.
18 A. C. Curtis, D. G. Duff, P. P. Edwards, D. A. Jefferson, B. F. G. Johnson, A. I. Kirkland and A. S. Wallace, *J. Phys. Chem.*, 1988, **92**, 2270–2275.
19 J. Khatouri, M. Mostafavi, J. Amblard and J. Belloni, *Chem. Phys. Lett.*, 1992, **191**, 351–356.
20 P. Mulvaney, in *Nanoscale Materials in Chemistry*,ed. K. J. Klabunde, John Wiley & Sons, Inc., New York, 2001, pp. 121–167.
21 R. M. Tilaki, A. Irajizad and S. M. Mahdavi, *Appl. Phys. A*, 2007, **88**, 415–419.
22 R. Šípoš, T. Z. Szabó-Plánka, A. Rockenbauer, N. V. Nagy, J. Šima, M. Melník and I. N. Nagypál, *J. Phys. Chem. A*, 2008, **112**, 10280–10286.

23 G. F. Smith and W. H. Mccurdy, *Anal. Chem.*, 1952, **24**, 371–373; S. Goldstein and G. Czapski, *Inorg. Chem.*, 1985, **24**, 1087–1092.
24 R. D. Gray, *J. Am. Chem. Soc.*, 1969, **91**, 56–62; L. Mi and A. D. Zuberbuhler, *Helv. Chim. Acta*, 1992, **75**, 1547–1556.
25 K. Sivakumar, F. Xie, B. M. Cash, S. Long, H. N. Barnhill and Q. Wang, *Org. Lett.*, 2004, **6**, 4603–4606; F. Alonso, Y. Moglie, G. Radivoy and M. Yus, *Eur. J. Org. Chem.*, 2010, 1875–1884; F. Alonso, Y. Moglie, G. Radivoy and M. Yus, *Tetrahedron Lett.*, 2009, **50**, 2358–2362.

This journal is © The Royal Society of Chemistry 2013